



Long-term RFID SLAM using Short-Range Sparse Tags

Jiun-Fu Chen and Chieh-Chih Wang*

Department of Computer Science and Information Engineering, National Taiwan University, Taipei, Taiwan

(Received 12 August 2014; Accepted 19 November 2014; Published on line 1 March 2015)

*Corresponding author email: bobwang@ntu.edu.tw

DOI: 10.5875/ausmt.v5i1.843

Abstract: While on the path forward to the long-term or lifelong robotics, one of the most important capabilities is to have a reliable localization and mapping module. Data association and loop detection play critical roles in the localization and mapping problem. By utilizing the radio frequency identification (RFID) technology, these problems can be solved using the extended Kalman filter (EKF) based simultaneous localization and mapping (SLAM) with the tag information. But one of the critical barriers to the long-term SLAM is the overconfidence issue. In this paper, we focus on solving the overconfidence issue, which is introduced by the linearization errors. An Unit Circle Representation (UCR) is proposed to diminish the error in the prediction stage and a Correlation Coefficient Preserved Inflation (CCPI) is developed to recover the overconfidence issue in the update stage. Based on only odometry and sparse short-range RFID data, the proposed method is capable to compensate the linearization errors in both simulation and real experiments.

Keywords: Radio Frequency Identification (RFID); Simultaneous Localization and Mapping (SLAM); Long-term Robotics

Introduction

Simultaneous localization and mapping (SLAM) is one of the foundation stones for long-term robotics. The detection and recognition of the loop closures are critical in SLAM, in which the incorrect loop closures leads to bad estimates or divergence. Our previous work [11] has shown that loop detection can be solved by matching the tag ID directly. However, one of the remaining issues is overconfidence in which the ground truths of landmarks are not properly covered by the estimates.

The overconfidence situation, also called inconsistency, is difficult to compensate, due to that the ground truth is impractical to obtain in real environments. Thus, the inconsistency detection and recovery are almost impossible without any further information. The inconsistency could be introduced by the linearization error while obtaining the first order derivative approximation [17]. In this paper, a modification of the state vector representation, the unit circle representation, is applied to decrease the linearization errors. Moreover, in order to recover from the inconsistency, an inflation scheme, the correlation

coefficient preserved inflation, is utilized to enlarge the possibility of the estimates while considering the relationships between landmarks and the robot. With these two improvements, the residual of the first order derivative approximation can be compensated for performing long-term SLAM. Following our previous work [11], a short-range passive RFID system is exploited to accomplish a low cost and highly reliable long-term SLAM system.

It is well known that the RFID technology is flexible and feasible because of RFID's fast detection capability and contactless identification with perfect data association. The RFID technology has been used to solve a number of daunting robot perception problems such as mapping, localization and activity recognition. With a predefined or calibrated map of RFID tags, localization can be performed [3-5]. Hähnel *et al.* [6] and Joho *et al.* [7] proposed to learn the map of the RFID tags with perfect localization, and then use the built map to perform localization in which mapping and localization are solved separately in two stages. In [8], data from a camera and RFID mounted on a pan-tilt unit of a robot are fused to accomplish person tracking in which a RFID tagged person can be followed by the robot.



Our previous work [11] has demonstrated the feasibility of using RFID to solve the data association problem. It was pointed out that there are three major differences comparing to the conventional EKF-based SLAM with laser scanners. The first one is the contrast between the large odometry uncertainty and the small RFID sensor uncertainty. The huge odometry uncertainty is increased continually as the robot moves while the uncertainty from the RFID is within a 10 cm radius circle. The second one is that if a local RFID measurement is obtained, the localization is accurate. Since the sensor model is accurate, the localization of the robot near the tags is precise due to that the uncertainty of the robot converged quickly to the landmark/tag. The final one is that the update step is executed less frequently. While operating in environments with sparse tags, only the prediction step is executed in most of the time. Therefore, one of the challenges of EKF-based RFID SLAM is to estimate the robot pose between the tags.

As the previous work, we utilized the low-end sensor, RFID, to perform a reliable SLAM while verifying the proposed ideas. Figure 1 (a) shows the NTU-PAL4 robot in which the RFID reader was mounted on the right side of the robot and the SICK LMS291 laser scanners were used to collect ground truth data. Figure 1 (b) shows the RFID system used in this work. The RFID system is the RWM600 module for ISO/IEC 15693 spec working on 13.56MHz channel with 5Hz reading frequency and the sensible range is 0.1 m. As the RFID devices in this work only have a centimeter level of detection range, only odometry data are available most of the time in the situations that RFID tags are deployed sparsely in environments. While a new feature/landmark is added to the SLAM state vector, the global pose uncertainty of the robot is taken into account to estimate the location probability of this new feature. Since the deployed tags are sparse, the size of the SLAM state vector can be maintained for real time applications

Jiun-Fu Chen received his B.S. and M.S. degree from Computer Science and Information Engineering at National Taiwan University in 2007 and 2012, respectively. He is currently a Ph.D. student at the Robot Perception and Learning Laboratory at National Taiwan University. His research interests include long-term robotics, simultaneous localization and mapping, and dynamic scene understanding.

Chieh-Chih (Bob) Wang earned his Ph.D. in Robotics from the School of Computer Science at Carnegie Mellon University in 2004. He received his B.S. and M.S. from National Taiwan University in 1994 and 1996, respectively. During his graduate study, he worked with the Bayesian vision group at the NASA Ames research center and at Z+F Inc. in Pittsburgh. From 2004 to 2005, he was an Australian Research Council (ARC) Research Fellow of the ARC Centre of Excellence for Autonomous Systems and the Australian Centre for Field Robotics at the University of Sydney. In 2005, he joined the Department of Computer Science and Information Engineering at National Taiwan University, where he is an Associate Professor and is pursuing his academic interests in robotics, machine perception and machine learning. Dr. Wang received the best conference paper award at the 2003 IEEE International Conference on Robotics and Automation (ICRA).

with limited computational resources.

Note that the interference between RFID antennas should be introduced to any RFID system with multiple readers. In this work, only one RFID antenna is exploited to reduce the complex interference issue. Still, the RFID system used in this work shows the existence of a tag while this tag has left the sensible area of the reader from a couple more seconds ago. Unlike [26] to learn the probability of the detection correctness, the delayed-state EKF [8] is implemented to deal with the false measurements to diminish the effect.

With the remove of false measurements, a modification of the state vector representation, and a technique to adjust the estimate while considering the relationship between the robot and landmarks, a long-term RFID SLAM can be demonstrated. The following sections of this paper are organized as the following. Sec. II describes the related works on the RFID sensor model and the modifications to improve EKF SLAM. The vanilla EKF RFID SLAM approach, the unit circle representation in the prediction step, and the correlation coefficient preserved inflation in the update step are introduced in Sec. III. Sec. IV exhibits the simulation results in different conditions. Sec. V shows the results of the real experiments. In the end, Sec. VI concludes the contributions of this work.



(a) The NTU-PAL4 robot.



(b) The short-range passive RFID reader and tag.

Figure 1. The RFID system is mounted on the right side of the NTU-PAL4 robot parallel to the robot body. The SICK laser scanners on the top of the robot were used to collect ground truth data.

Table 1. Comparison of the related works. In the tag layout item, R is the abbreviation of *random* and S stands for *structured* in which the type of deployment is specified. In the number of tags column, *Active* indicates the active RFID system is used.

Approaches	Achieved Task	Tag Layout	Antenna (Reader)	Detection Range (m)	#Tags	Field Size	Coverage (m ² /tag)
Hähnel <i>et al.</i> [4]	Mapping first, then Localization	R	2	6	100	28m*28m	7.84
Joho <i>et al.</i> [5]	Mapping first, then Localization	R	2	5	350	1m between 2 tags	1
Ni <i>et al.</i> [1]	Localization only	S	4	45	16 Active	4m*9m	2.43
Liu <i>et al.</i> [2]	Localization only	R	2	10	30	4m*10m	4
Bohn and Mattern [3]	Localization only	S	1	0.04	30	0.5m*0.5m	0.0083
Johansson and Saffiotti [9]	Navigation, Mapping	S	1	1	350	7m*4m	0.08
Vorst and Zell [10]	Trajectory estimation	R	4	10	400	15m*10m	0.375
Kleiner <i>et al.</i> [7]	Exploration, SLAM with laser	R	1	0.3	50	16m*16m	5.12
Chen and Wang [11]	SLAM	R	1	0.1	25	20m*50m	40
Artur and Zell [26]	Mapping, negative information	R	2	7	71	65m ²	0.915

Related Work

Table 1 summarizes a comparison of the related works and demonstrates the significance of the approaches in terms of the cost, the achieved tasks and the coverage area per tag. While most works use long-range active or passive RFID technology and deploy dense tags on the scene to accomplish localization and mapping separately, our previous work [11] has been employed to show with sparse tags as the conventional approach in this work. For RFID systems, there are two major measurement modeling approaches, the environment based model and the sensor centric model. In the environment based modeling approach, data are collected at each place in the environment as snapshots or fingerprints [12][13] which are later used for accomplishing localization. In [10], the robot trajectory is estimated in a batch-processing fashion which could be unsuitable for real-time and online robotic applications. The sensor centric measurement modeling approach was firstly proposed in [6]. Vorst and Zell [14] proposed a semi-supervised learning approach to learn about the detection probability. With a high-end long-range RFID system, Ni *et al.* [3] adjusted the power levels of the antenna to change detection ranges for estimating distances between the reader and tags. In the RFID systems that the received signal strength indication (RSSI) is available, the signal strength can be used for estimating distances between the reader and tags [15]. Joho *et al.* [7] took both RSSI and the detection probability into account using a hybrid measurement model. With the high-end RFID systems, measurements from RFID could contain range information. And with multiple readers, bearing information could be available. In this work, a low-end RFID system is applied in which both range and bearing information are unavailable.

For sensors which are not capable to obtain the measurement information instantly, the delayed

initialization method is applied for waiting more confident data or accumulating the range data from two bearing only measurements. In the control literature, the delayed-state EKF had been proposed to estimate the states of nonlinear time-delay systems [8]. In the robotics literature, Eustice *et al.* [16] used the exactly sparse delayed-state filter to initiate new landmarks. With the augmented poses, landmarks can be estimated more accurately by exploiting delay measurements.

Julier and Uhlmann [17] exhibited a simple example that even the robot is stationary without any transition noise, the SLAM algorithm yields an inconsistent map subsequently in which the SLAM is utilized under a two-dimensional plane with a typical range-bearing sensor. The results of [17] show that the inconsistency issue is introduced by the non-linear model. Following this conclusion, Castellanos *et al.* [18] reexamined the same problem and find out that the inconsistency from the linearization error would make the estimator overconfident after a long duration or in a large environment. Therefore, [18] suggests keeping the small map and applies a local map solution to their following work [19].

Bailey *et al.* [20] and Huang and Dissanayake [21] take a further look of the inconsistency phenomenon. Bailey *et al.* [20] learn that the vehicle heading uncertainty is the major cause of the inconsistency problem in 2D SLAM. Furthermore, [20] provides a verification index called Normalized Estimation Error Squared (NEES) to characterize the filter performance. Huang *et al.* [21] interpret the convergence property and the source of inconsistency with theoretical proofs which support that the scale of the angular uncertainty would affect the inconsistency as discussed in [20]. Moreover, [21] provide the lower bound of the uncertainty for the 2D SLAM problem which constructs the connections between the theoretical stationary uncertainty and the given motion and observation models.

Accordingly, the conventional EKF SLAM would be



inconsistent in large environments. Castellanos *et al.* [19] use small robo-centric maps to reduce the expansion of the nonlinearity, but the fundamental problem of the inconsistency still exists. Agamennoni *et al.* [22] propose an outlier robust Kalman Filter to remove outliers and reduce the inconsistency. [22] focuses on dealing with sequential data in which the non-Gaussian and heavy-tailed noise occurs. The key idea of [22] is applying a recursive iteration to execute the update step of the EKF several times. By adjusting the sensor uncertainty, the update step would converge with robustness. Since there is a recursive step in the update step, the computational cost would be higher than the conventional method. Choi and Oh [23] proposed to inflate the covariance matrix according to the shifted mean to deal with the so-called "disturbance". Thus, the Shifted Mean based Covariance Inflation (SMCI) is utilized to expand the covariance matrix to cover the disturbance as one of the possibility. But the drawback of the SMCI method is that the relationships between the robot and landmarks are not taken into consideration.

Long-term RFID SLAM

The framework to achieve long-term RFID SLAM is based on our previous work [11]. Then, since the previous work will failed to perform long-term tasks, we proposed two improvements in the prediction and update stages of the EKF estimator. The first modification focuses on the prediction step of the EKF to improve the linearity while the second modification aims at the update step of the EKF to increase the robustness while overconfidence happened.

Vanilla Approach and Essential Probabilistic Models

The EKF estimator is utilized to compute the estimate following the scheme in [11]. The robot pose in the global coordinate system is computed with data from odometry given the initial pose. The robot pose transformation is the same as [24] in which the pose is represented with $[x \ y \ \theta]$ as a point with orientation. Therefore, the odometry information is decomposed to three components: a rotation, followed by a straight line translation, and another rotation to finalized one step movement. The motions are formulated as a $[d \ r1 \ r2]$ vector, in which d is the translation, $r1$ is the initial rotation, and $r2$ is the final rotation. Following [24], the probability is represented with a Gaussian distribution. Therefore, the variances of the three components are estimated using:

$$\sigma_d^2 = \begin{cases} \sigma_{d,min}^2 & ,if \alpha * d < \sigma_{d,min} \\ (\alpha * d)^2 & ,otherwise \end{cases} \quad (1)$$

$$\sigma_r^2 = \begin{cases} \sigma_{r,min}^2 & ,if \beta * (r1 + r2) < \sigma_{r,min} \\ \frac{(\beta * (r1 + r2))^2}{2} & ,otherwise \end{cases}$$

where α and β are the percentage of the distance and rotation difference and $\sigma_{d,min}$, $\sigma_{r,min}$ are the minimum standard deviation of distance and rotation respectively.

The probabilistic short-range RFID measurement model is established as $P(z_t | \Delta(x_t; l_i))$, where $\Delta(x_t; l_i)$ is the relative location between the i -th tag and the RFID antenna, z_t is the measurement from the reader, x_t is the antenna pose, and l_i is the i -th tag location. Without RSSI and power level data, our RFID system only receives strings of the tag ID code. Therefore, the nearby 2D space is separated to 2cm by 2cm grids and accumulated the tag detection events respectively. The weighted mean and variance with respect to the antenna coordinate system are computed by utilizing the histogram of the tag detection events in a 2D space.

More than essential models in the vanilla approach, our RFID system shows that some ghost detection exist during the detecting period as describing in [26]. The tag arriving events are sensitive and accurate in which the measurement delay is less than 0.2 seconds. Unfortunately, the tag leaving events response much more slowly and the delays can be up to 1.6 seconds. This means that the reader still reports the existence of a tag while the tag has already left the sensible area of the antenna. These incorrect measurements would produce incorrect estimates of the tag locations. Thus, the delayed time should be modeled to compensate the effects. By considering the temporal and spatial relationships between the tag and the antenna, the tag location in the antenna coordinate system transferred to the global coordinate system with compound and inverse transformations.

To compensate this delay effect, a queuing method is introduced to recover the leaving measurements. The measurements from the time of tag leaving to the previous 1.6 seconds are removed in the measurement queue. With the use of delayed-state EKF [16], the augmented poses are activated when the tags are observed with collecting the poses of the delayed measurements. In this work, at most 10 augmented poses are kept and will be eliminated while there is no new observation. With these 10 augmented poses, the proposed method would be guaranteed to cover 2 seconds comparing to the 1.6 seconds time delay. Here, the augmented poses are introduced to estimate the



SLAM state with:

$$\begin{aligned}
 &P(X_t, M | Z_{t-k}, U_t) \\
 &= \underbrace{P(x_t | x_{t-1}, u_t) \cdots P(x_{t-k+1} | x_{t-k}, u_{t-k+1})}_{\text{Augmented poses}} \times P(x_{t-k}, M | Z_{t-k}, U_{t-k})
 \end{aligned}
 \tag{2}$$

where $X_t = x_{t:k:t}$, $Z_{t,k} = z_{1:t-k}$, $U_t = u_{1:t}$ and M are the robot state, measurements, control commands and estimated map respectively. k is the delayed time of the measurement. From (2), the robot trajectory from time $t-k$ to time t is saved. The augmented poses with a sliding window scheme are applied when the new tag measurement arrived and the augmented poses are removed from the current state vector if there is no measurement.

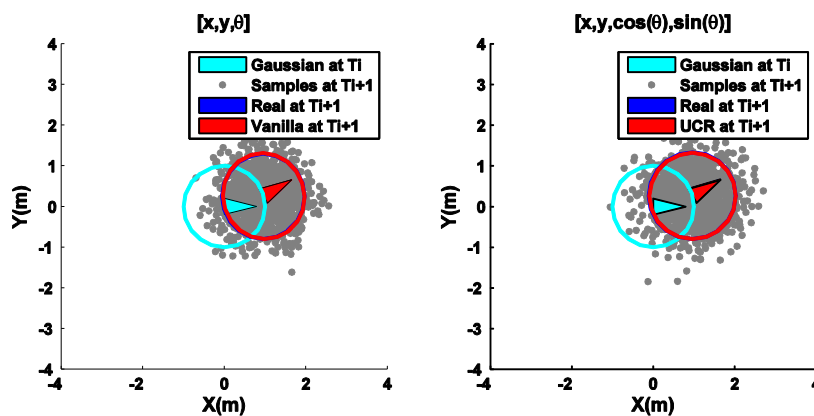
Linearization Improvement with Unit Circle Representation (UCR)

The nonlinearity would cause the EKF estimator to become overconfidence which would lead to a diverged estimate. By examining the EKF equations, the linearization error is introduced by not only the transformed control noise, but also the transition Jacobian. Figure 2 reveals two situations with small and large uncertainty under the perfect motion control assumption which represents that the control noise is zero. It is obviously to show that even under the perfect motion control assumption; the robot pose uncertainty would introduce large linearization error if the original value of the uncertainty is large. That is because of the transition is not linear due to the heading of the robot.

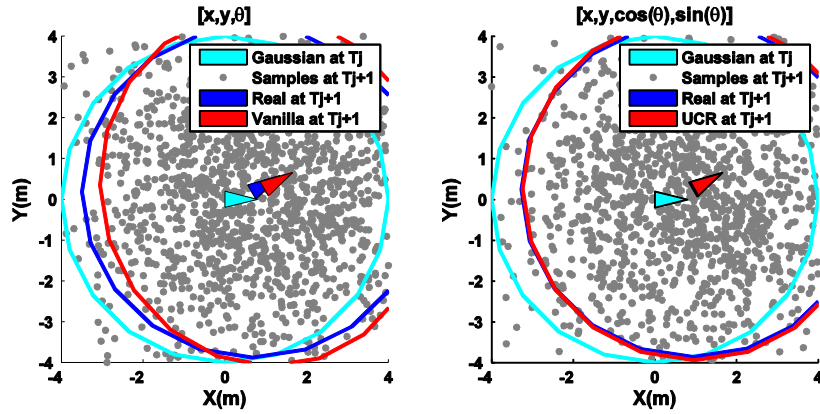
Therefore, the objective of the modification here is to make the transition as linear as possible.

A well-known linear transformation in the Computer Graphics literature is the Quaternion transformation at the three dimensional space. We first applied the Quaternion on the 2D space with the projection. Unfortunately, the Quaternion projected to two dimensional space is not linear while performing the transition. Two quadratic terms are generated during the transition and lead to nonlinear. By employing the Angle Addition Theorems, the quadratic terms are eliminated and the representation of the robot pose is Equation (3). Therefore, the prediction transition is Equation (4).

The relationship between the proposed unit circle representation and the θ only representation is a projection from the θ domain to the 2D space composed with cos and sin functions. It is clear that the proposed representation makes a projection to a unit circle (cos, sin). From Table 2, the linearity of two angular space representations are compared. The representation of θ is linear at the dimension of θ , but it is nonlinear at the dimension of x and y since the cos and sin functions provide the nonlinear transform here. The proposed unit circle representation is linear at all dimensions of the robot state. The unit circle representation can reduce the nonlinearity as shown in Figure 2. In Figure 3, the area of the ground truth distribution covered by the estimator is revealed with different angular uncertainty. After 25 degree uncertainty, the proposed approach covered more area than the vanilla approach. The result is generated with 15000 samples and 2 m uncertainty in x and y .



(a) Small uncertainty situation. The left figure is the vanilla approach while the right figure is the proposed approach with 2σ bound



(b) Large uncertainty situation. The left figure is the vanilla approach while the right figure is the proposed approach with 2σ bound

Figure 2. Different situations under the perfect control assumption. When the uncertainty of the robot is small at T_i , the prediction from T_i to T_{i+1} introduced quite small linearization error in which could be negligible. But if the uncertainty of the robot is large, the prediction from T_j to T_{j+1} led to huge linearization error.

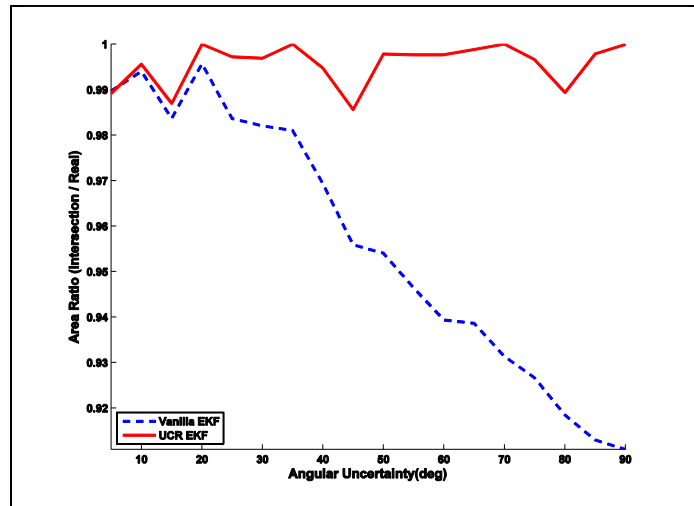


Figure 3. Area covered by the estimators to the ground truth.

Table 2. Comparison between different angular representations. Note that the control input of the odometry motion model is $(d, r1, r2)$ and the variables with prime is the prediction result at the next time step comparing to the variables without prime.

Angular representation	θ	$\cos(\theta), \sin(\theta)$
Robot state	$(x, y, \theta)^T$	$(x, y, \cos(\theta), \sin(\theta))^T$ (3)
Transition formulation	$\begin{pmatrix} x' \\ y' \\ \theta' \end{pmatrix} = \begin{pmatrix} x + d * \cos(\theta + r1) \\ y + d * \sin(\theta + r1) \\ \theta + r1 + r2 \end{pmatrix}$	$\begin{pmatrix} x' \\ y' \\ c' \\ s' \end{pmatrix} = \begin{pmatrix} 1 & 0 & d * \cos(r1) & -d * \sin(r1) \\ 0 & 1 & d * \sin(r1) & d * \cos(r1) \\ 0 & 0 & \cos(r1 + r2) & -\sin(r1 + r2) \\ 0 & 0 & \sin(r1 + r2) & \cos(r1 + r2) \end{pmatrix} \begin{pmatrix} x \\ y \\ c \\ s \end{pmatrix}$ (4)

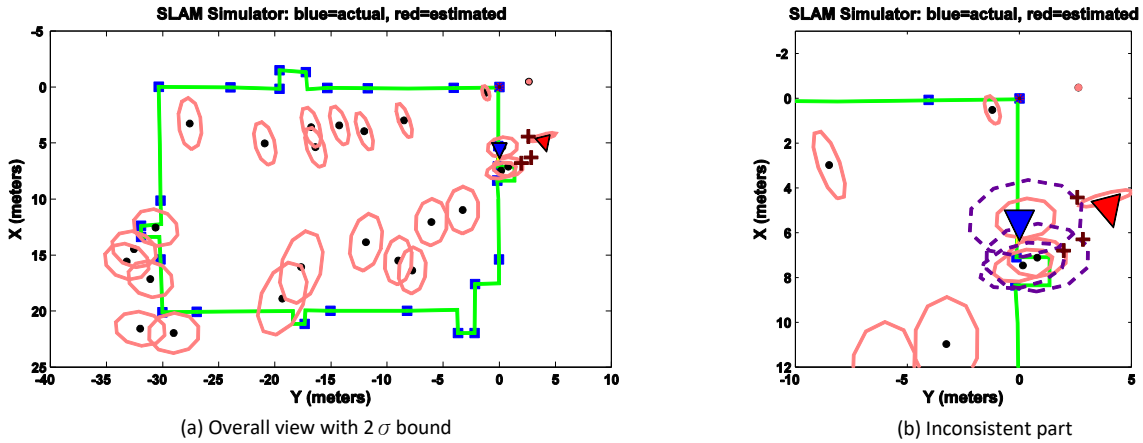


Figure 4. Overconfidence case with 25 tags. The blue squares are the ground truth of tags while the black dots are the estimation with the two sigma bound uncertainty colored with light red ellipses after the prediction step. The green line is the desired robot path. The brown crosses are the target points which the inflated covariance needs to cover. The purple ellipses on the right figure are the inflated covariance according to the target points.

Robustness Improvement with Correlation Coefficient Preserved Inflation Techniques (CCPI)

Since the times of the prediction is much larger than the times of the update in our setting, the overconfidence issues are significant as shown in Figure 4. This case shows that the overconfidence could happen at loop closures. The overconfidence can be recovered by inflating the uncertainty, with directly multiply a factor or [23] to compensate the residuals.

Instead of the naive method which enlarges the whole covariance matrix with a single factor, we proposed a scheme with different inflating factor while considering the correlation coefficient between landmarks and the robot. Since the related correlation terms are one of the most important elements in the EKF, we should modify the correlation terms according to the correlation coefficient to preserve the relationship between landmarks and robot while performing covariance inflation. The correlation coefficient between two variables is rewritten as:

$$\rho_{X,Y} = \text{corr}(X,Y) = \frac{\text{cov}(X,Y)}{\sigma_X \sigma_Y} = \frac{\sqrt{\gamma_X} \sqrt{\gamma_Y} \text{cov}(X,Y)}{\sqrt{\gamma_X} \sigma_X \sqrt{\gamma_Y} \sigma_Y} \quad (5)$$

where γ_X and γ_Y are two desired inflating factor for X and Y accordingly. Thus, the relationship between landmarks and the robot can be preserved. Therefore, the matrix form of the inflating factor is:

$$\tilde{\Sigma}_t = A * \bar{\Sigma}_t * A^T \quad (6)$$

$$A = \begin{pmatrix} \sqrt{\gamma_R} I_2 & 0 & 0_2 & \dots & 0_2 \\ 0 & \sqrt{\gamma_\theta} & 0 & \dots & 0 \\ 0_2 & 0 & \sqrt{\gamma_{l_1}} I_2 & \dots & 0_2 \\ \vdots & \vdots & \vdots & \ddots & \vdots \\ 0_2 & 0 & 0_2 & \dots & \sqrt{\gamma_{l_n}} I_2 \end{pmatrix} \quad (7)$$

where A is the inflating matrix with n landmarks, 0_2 is a 2 by 2 zero matrix, I_2 is a 2 by 2 identity matrix, γ_R is the inflating factor of the robot pose, and γ_θ is the inflating factor of the robot orientation. If the robot pose is represented by the unit circle representation, the inflating factor of the angular information would be separated to \cos and \sin space respectively. For example, the inflating factor γ_{li} of the i -th landmark is:

$$\gamma_{li} = \frac{(\mu_{li} - \bar{\mu}_{li})^T \bar{\Sigma}_{li}^{-1} (\mu_{li} - \bar{\mu}_{li})}{\lambda^2} \quad (8)$$

where μ_{li} is the mean after the update, λ is the desired inflation sigma bound and $\bar{\mu}_{li}$ and $\bar{\Sigma}_{li}$ are the mean and covariance matrix after the prediction respect to i -th landmark. The proposed inflating factor varies according to the update mean and the predicted estimation. By applying Equation (8) and Equation (6), the correlation coefficient between each landmark and the robot are preserved.

Three covariance inflation methods are evaluated, including a naive method, Choi and Oh [23], and the proposed CCPI. Assuming the inflation factor is γ , the naive method to tackle the covariance inflation is by :

$$\tilde{\Sigma}_t = \gamma * \bar{\Sigma}_t \quad (9)$$

Figure 5(a) reveals the result using the naive method and it shows that once the inflation is performed,

it is hard to converge back. Another drawback of inflating the covariance with single factor is that there are some landmarks in which their inflations are unnecessary. Therefore, by applying [23], Figure 5(b) exhibits the inflated result. It is better than the naive inflation scheme, but it is still could not converge as the

relationship between the robot and each landmark is not taking into account. The result of the proposed inflation scheme is displayed in Figure 5(c), which show that after preserving the relationship, the estimate can converge better and more accurate.

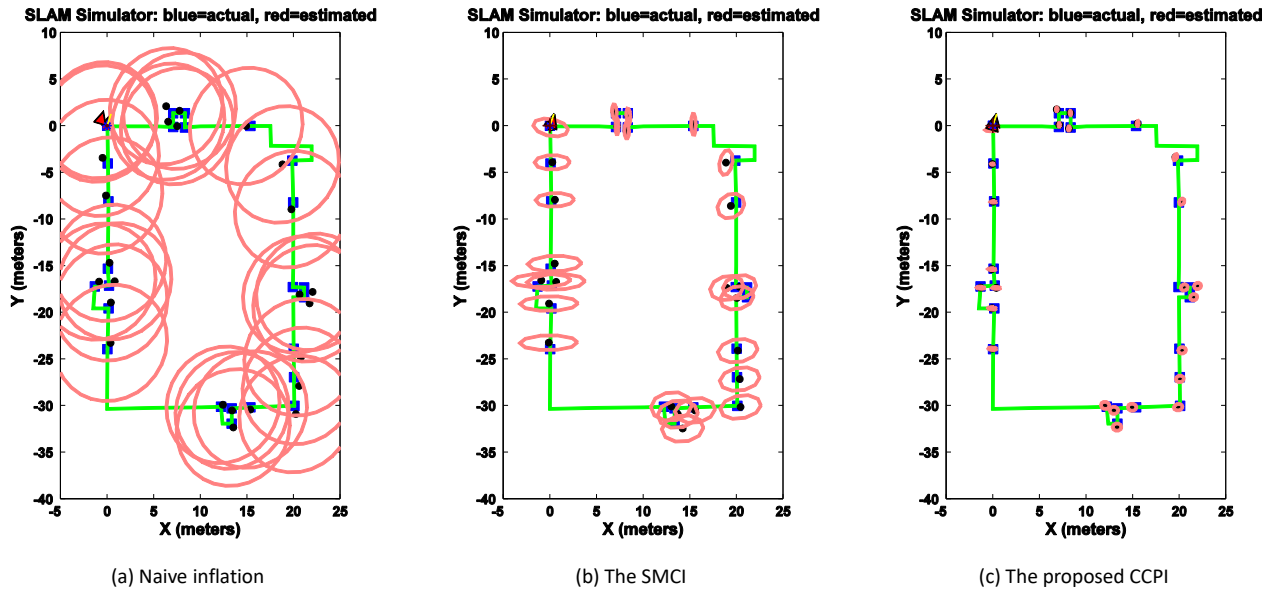


Figure 5. The results of three inflation methods with 25 tags after 10 loops with 2σ bound

Evaluation with Simulations

To evaluate the improvements, we define the evaluation metric for analysis. Since the modification for the long-term RFID SLAM is not only about the mean positions of tags and the robot pose but also about the related covariance matrix, Euclidean distance (E-dist) and Mahalanobis distance (M-dist) are applied for the performance quantitatively. The detection range of the RFID antenna is 10 cm in all simulations. The simulated robot equipped with one RFID antenna mounted in front of the platform. The simulation environment is 30m×20m with 40 tags deployed randomly along the path. As the proposed approach using RFID and odometry data has limited bearing information, the results often show an angular shift compared to the ground truth. To properly evaluate the performance, the results are aligned with the ground truth with perfect tag ID association using the iterated closest point (ICP) algorithm [25].

Analysis with the Different Improvements

In the first simulation, the effects of different improvements are evaluated with 25 tags. The combinations of the improvements are vanilla EKF SLAM, unit circle representation, correlation coefficient

preserved inflation with the vanilla EKF SLAM, and applying both proposed modifications. Figure 6 shows the mapping accuracy of different kinds of improvements with 25 tags along the number of loops. The results indicate that the unit circle representation causes small improvement while the correlation coefficient preserved inflation introduces large improvement. Another observation from the results is that both indices are decreased along time gradually. The results in Figure 6 also illustrate that the M-dist is lower for the method with the proposed inflation technique in which the technique leads to the better estimates.

Besides, the performance of the robot localization is also verified with the E-dist and M-dist as shown in Figure 7. Since the best performance is obtained with applying both improvements, the figures only display the difference of the both applied method and the conventional approach. And the proposed method reduces the robot localization error as the results reveal in the mapping in Figure 6.

For detailed statistic values, we list the average E-dist in both localization and mapping at Table 3. The average E-dist of the localization is computed after the first loop closure while the E-dist of the mapping is obtained from the result after the 10 loop trajectory. It shows that the proposed method improves the

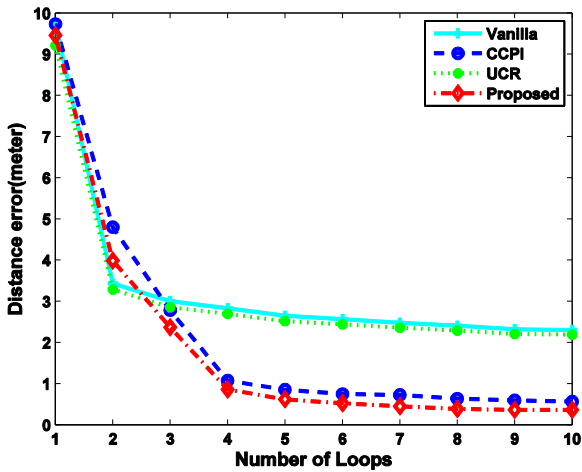
performance in both localization and mapping.

In addition to the numerical comparison, the whole results after the 10 loop journey are illustrated in Figure 8. As illustrated in Figure 6, the same conclusion is confirmed that the improvement of the unit circle representation is smaller than the correlation coefficient preserved inflation. And still, the results with both improvements are the best. From those figures, the upper results without the inflation technique encounter

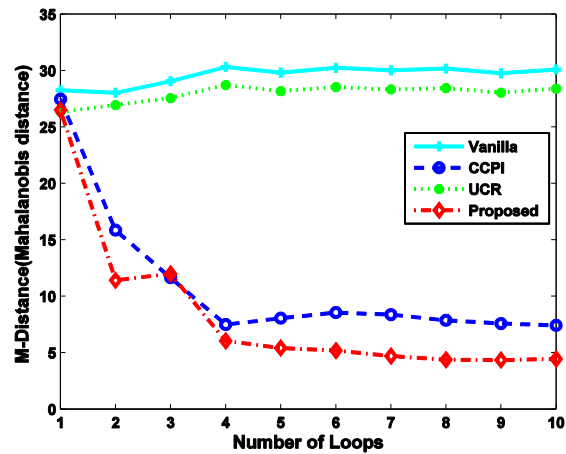
the overconfidence and could not compensate the effect while the lower results are capable to alter the uncertainty and lead to the proper estimate.

Table 3. E-dist comparison of the proposed method and the vanilla method in terms of robot localization and mapping.

	Robot Localization		Tag Mapping	
	Vanilla	Proposed	Vanilla	Proposed
25 tags	3.23m	1.91m	2.30m	0.36m

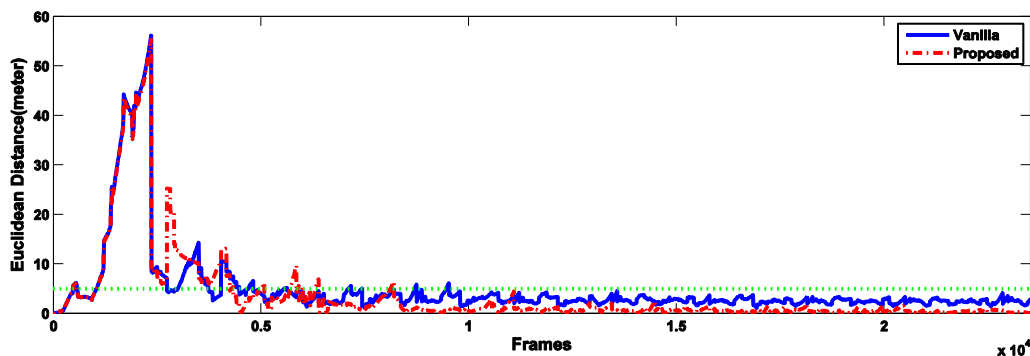


(a) E-dist of 25 tags in terms of mapping.

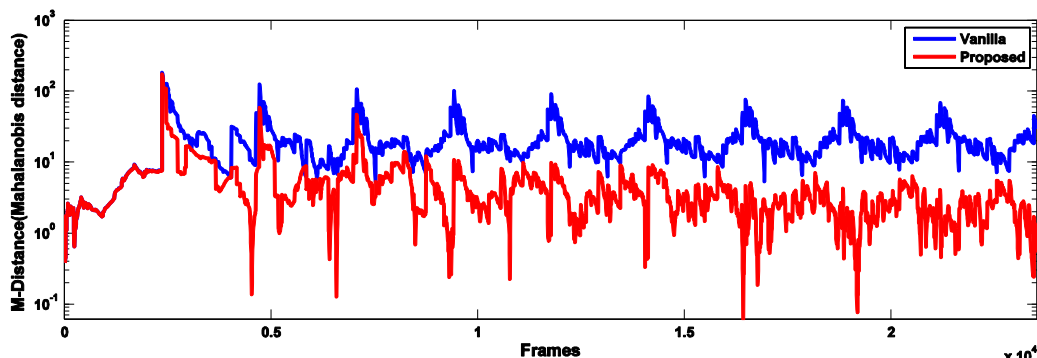


(b) M-dist of 25 tags in terms of mapping.

Figure 6. Mapping results of 25 tags.

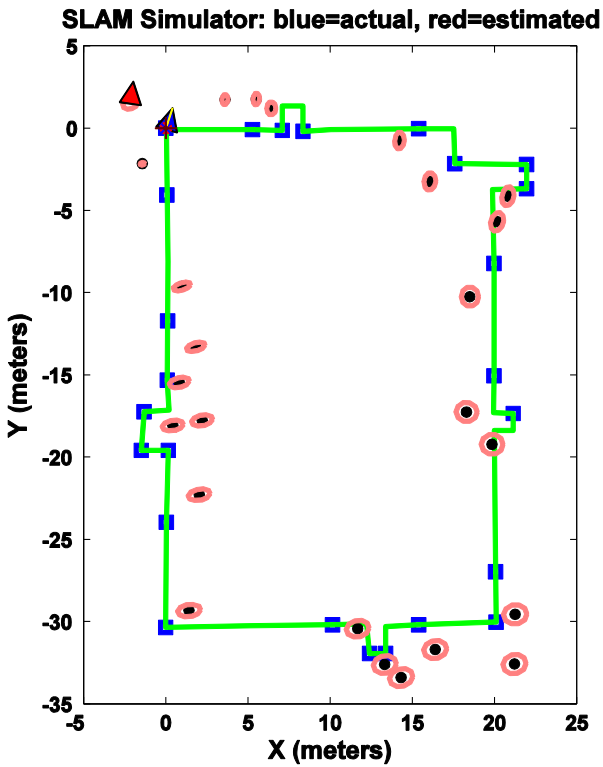


(a) E-dist of 25 tags in terms of robot localization.

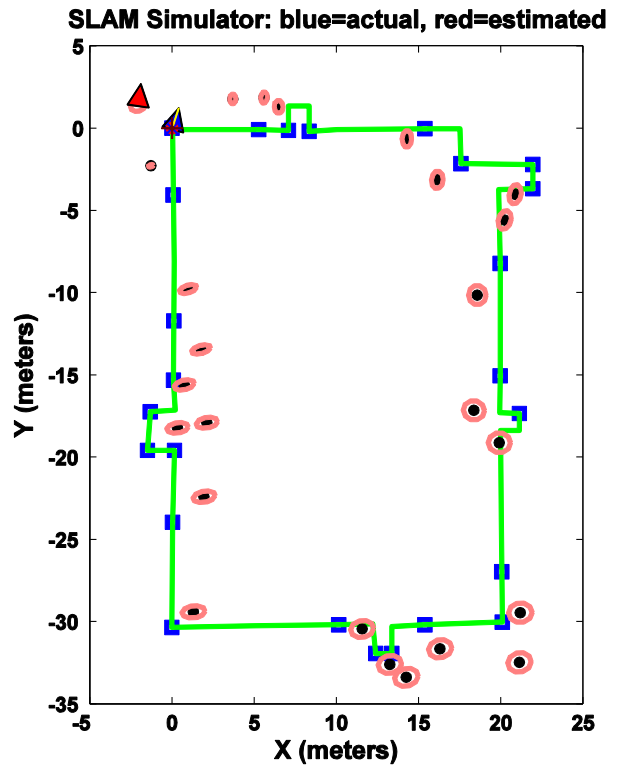


(b) M-dist of 25 tags in terms of robot localization.

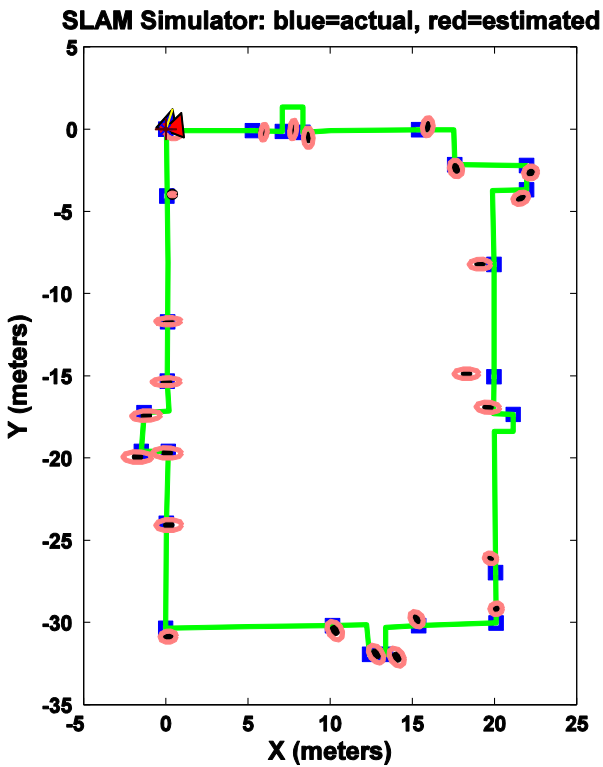
Figure 7. Localization E-dist and M-dist results of different improvements with 25 tags. The green dash line indicates the 5m error line for comparison.



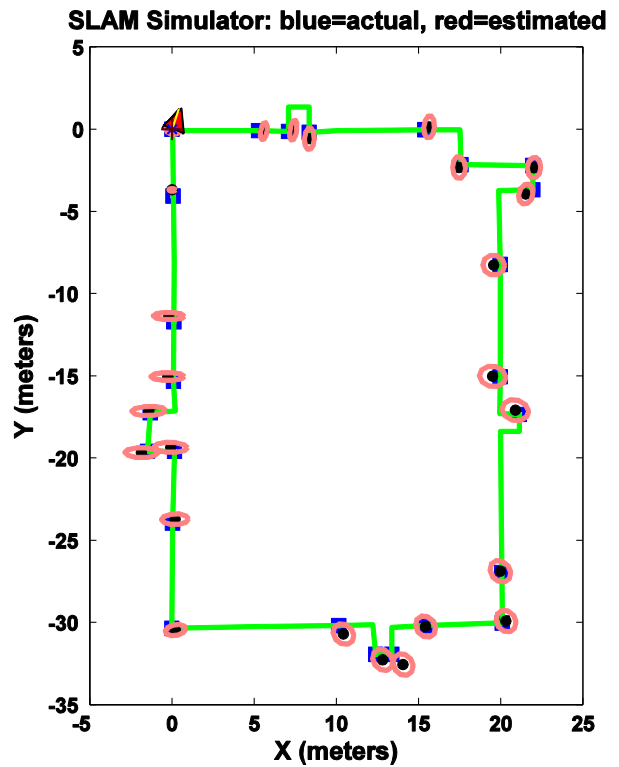
(a) Vanilla EKF-based SLAM



(b) UCR



(c) CCPI



(d) Applying Both Improvements

Figure 8. Simulation results of 25 tags after the 10th loop. The blue squares are the truth and the green line is the path in which the robot follows. The estimation results are the black dots with the light red ellipses of the mean and 5σ uncertainty bound.

Analysis with Monte Carlo Runs

The second simulation is the applicability of the tag distribution. Since EKF-based RFID SLAM is a data driven approach in which the different given data would have different outcomes, a Monte Carlo Test is applied to evaluate the performance of the proposed method under different tag distributions. This simulation performs 10 loops for each sample and applies Monte Carlo test with multiple samples for 7, 13, and 25 tags. In each sample, a given number of tags from the total 40 tags are selected randomly in the simulation. Table 4 shows the total Monte Carlo samples in this simulation. In Table 4, the cases of the vanilla approach are acquired from the mapping results while the improvement of the proposed method is verified with the E-dist and M-dist. If the estimate is larger than 3σ , the related tag is called overconfidence. Once over 50% of the landmarks are overconfidence, the sample is classified as the overconfidence case. Therefore, the criterion is stricter than [11] and nearly 50% of the samples are overconfidence. The statistics data in Table 4 reveals that the proposed method improves the percentage of the consistency case to more than 68% in all samples.

In order to understand the enhancements of the proposed method quantitatively, we verified the E-dist in both localization and mapping with the overconfidence cases after applying the vanilla approach and listed in Table 5. The localization result is computed the average error after the first loop closure and the mapping result is the average error of the tags at the 10-th loop closure. The results show that the improvements in the overconfidence cases are about 20 to 30 percent. Second, if the number of tags is higher, the E-dist is smaller in terms of the robot localization. This leads the conclusion that the more tags, the more accurate robot localization. But in terms of mapping, it points out the same conclusion that more tags do not always improve the performance as [11]. Because the path of the simulation is a rectangle and the estimator with fewer tags cases almost adjust the relationships in inter-sides rather than the relationships in intra-side. The results show that the proposed method is capable to tackle the overconfidence situation and increases the localization and mapping accuracy.

Table 4. Overall Monte Carlo Sample in different kinds of tag numbers. Once over 50% of the landmarks are overconfidence, the sample is classified as the overconfidence case. The definition of the over confidence here is the estimate is larger than 3σ .

7 tags(70 samples)		
	Vanilla	Proposed
Consistency	24(34.0%)	48(68.6%)
Overconfidence	46(66.0%)	22(31.4%)
13 tags(60 samples)		
	Vanilla	Proposed
Consistency	31(51.7%)	46(76.7%)
Overconfidence	29(48.3%)	14(23.3%)
25 tags(60 samples)		
	Vanilla	Proposed
Consistency	23(38.3%)	45(75.0%)
Overconfidence	37(61.7%)	15(25.0%)

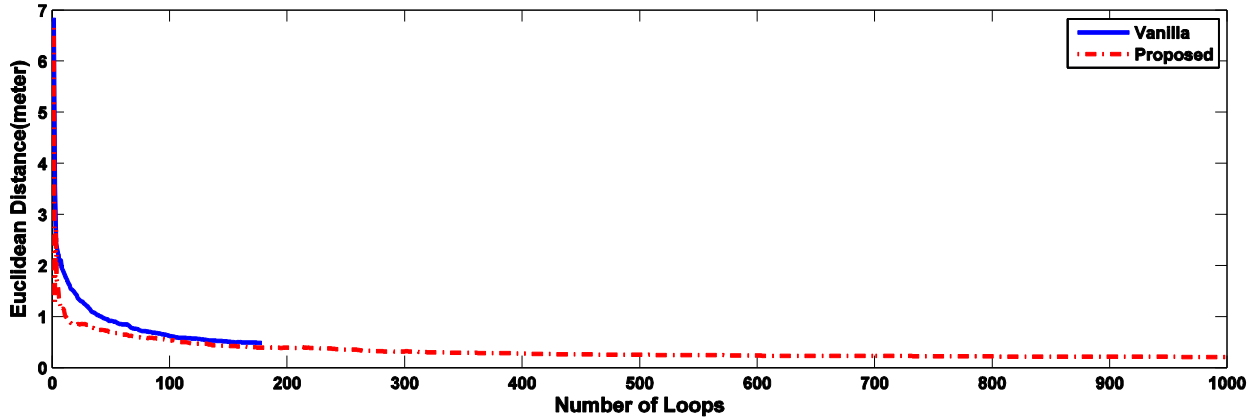
Table 5. E-dist comparison of the proposed method and the vanilla method in terms of robot localization and tag mapping of overconfidence cases.

	Robot Localization		Tag Mapping	
	Vanilla	Proposed	Vanilla	Proposed
25 tags(46 samples)	2.03m	1.47m (↓ 28%)	1.49m	0.69m (↓ 54%)
13 tags(29 samples)	2.66m	2.00m (↓ 25%)	1.45m	0.57m (↓ 61%)
7 tags(37 samples)	4.13m	3.40m (↓ 18%)	1.37m	0.79m (↓ 42%)

Analysis with Long-Term Capability

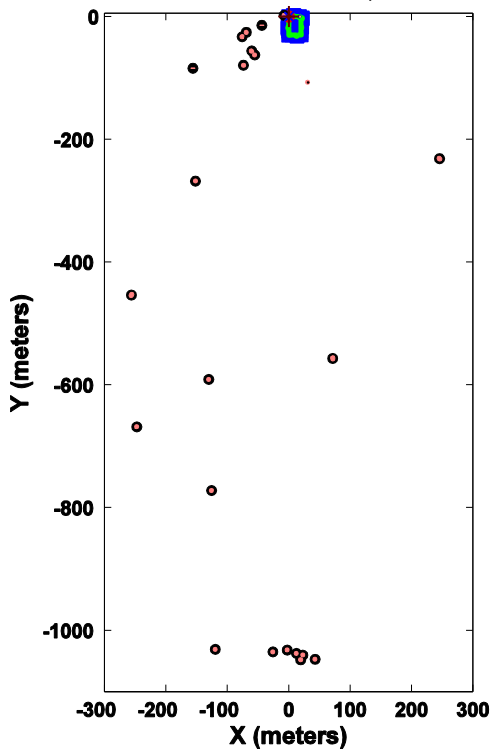
To test the long-term ability of the proposed approach, a simulation with 1000 loops using 25 tags is executed. Figure 9 reveals the mapping result after 1000 loops while Figure 9(a) is the E-dist of the comparison of the vanilla and proposed approaches. Note that the vanilla approach died after 178 loops. The result of vanilla approach in Figure 9(b) is the first diverged snapshot. The vanilla approach leads to overconfidence and the estimator crushed. Thus, Figure 9(a) illustrates that the proposed approach is survived after 1000 loops with a lower error than the vanilla approach. Moreover, the proposed method could adjust to a better estimate faster than the vanilla method in which the vanilla approach adjusted the estimate slowly. The result in Figure 9(c) illustrates that the proposed approach after 1000 loops is able to perform long-term slam with 0.21m Euclidean distance error.





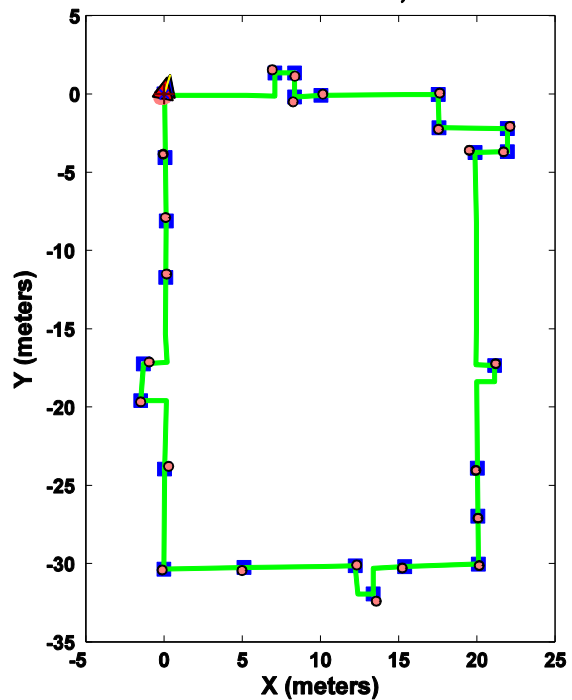
(a) E-dist in terms of mapping with 25 tags along 1000 loops.

SLAM Simulator: blue=actual, red=estimated



(b) Vanilla approach.

SLAM Simulator: blue=actual, red=estimated



(c) Proposed approach

Figure 9. The mapping results of vanilla approach after 178 loops and proposed approach after 1000 loops with 5σ bound. Note that the vanilla approach diverged and overconfidence to cover the ground truth.

Experiments using NTU-PAL4

The experiment using the NTU-PAL4 robot was conducted in 4th floor of the CSIE building in National Taiwan University. The environment size is about 20m by 50m and the 66 passive RFID tags were randomly attached on the wall. The NTU-PAL4 robot was controlled manually to follow the wall for tag detection and executed 4 loops in the environment. In this experiment, the result of using 25 tags which selected from the whole 66 tags is displayed. The mapping results are verified in which the ground truth is labeled manually

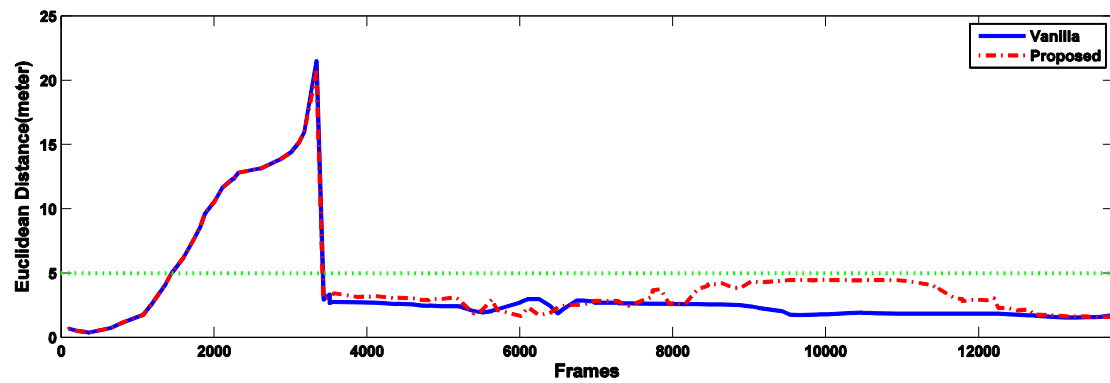
with the SICK laser scanner.

Figure 10 displays the mapping performance along the time steps. Figure 10 (a) and Figure 10 (b) exhibit the overconfidence recovery of the proposed method near the 10000 time step. The CCPI technique for recovery had been activated and the performance has been enhanced after several time steps. The dive of the final E-dist with 25 tags is from 1.70m using the vanilla approach to the 1.58m using the proposed method. The M-dist index in Figure 10 shows that the proposed method is more robust than the vanilla method while the M-dist value is usually lower in most of the time.

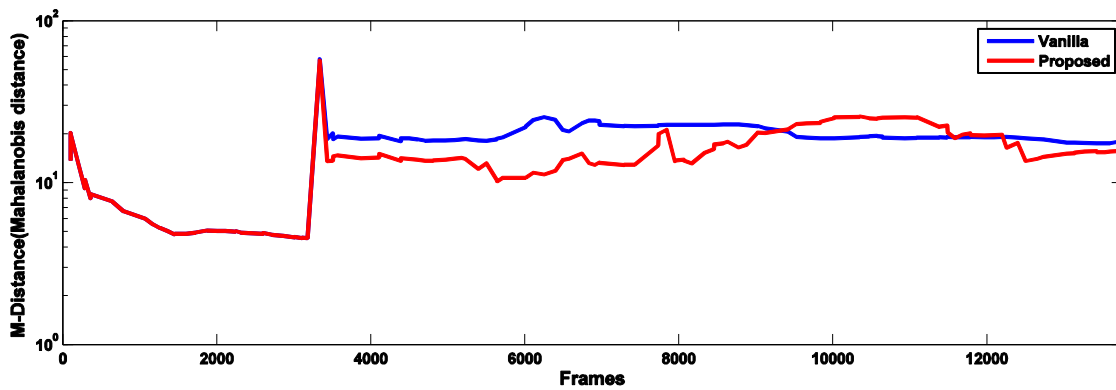
Furthermore, the final mapping results after 4 loop

closure are illustrated at Figure 11. Note that there is a large gap between two tags at the bottom of the map and this situation could not be handled in [11] and would introduce an oblique map in the end. The proposed method is capable of dealing this case and guides the estimate to the proper result. Since the experimental result is executed in 4 loops to demonstrate the trend,

the result of the estimate has larger uncertainty than the simulation cases. Through the real data experiments, the proposed method achieves that not only the topological geometry of the built map is still close to the ground truth, but also the overconfidence are endured and recover to a better estimate.



(a) Mapping E-dist of 25 tags.



(b) Mapping M-dist of 25 tags.

Figure 10. Mapping results of the real experiment along time with 25 tags. The green dash line indicates the 5m error line for comparison.



(a) Vanilla EKF-based SLAM. The E-dist of mapping is 1.70m.



(b) Proposed method. The E-dist of mapping is 1.58m.

Figure 11. Real experiment result of 25 tags after the 4th loop closure. The red triangle is the estimated robot pose and the black dots are the estimated tags with the light red ellipses 5σ bound. The blue squares are the ground truth labeling from the laser scanner data.

Conclusion

In this work, we proposed two improvements for the prediction and update step in the vanilla EKF-based RFID SLAM. The proposed modification could compensate the overconfidence and arrange the possibility to a proper estimate. Both simulations and experiments demonstrate that the proposed modifications are feasible while executing the long-term large-scale SLAM using short-range passive RFID with sparse tags. By applying the proposed techniques, the long-term RFID SLAM is feasible.

Acknowledgment

This work was supported in part by Ministry of Science and Technology of Taiwan and National Taiwan University under Grants NSC 103-2623-E002-010-D and MOST 103-2221-E-002-187.

References

- [1] L. M. Ni, Y. Liu, Y. C. Lau, and A. P. Patil, "Landmarc: Indoor location sensing using active RFID," in *Proc. of the IEEE int. conf. on pervasive computing and communications (PerCom)*, Los Alamitos, USA, pp. 407-415, 2003.
doi: [10.1109/PERCOM.2003.1192765](https://doi.org/10.1109/PERCOM.2003.1192765)
- [2] X. Liu, M. Corner, and P. Shenoy, "Ferret: RFID localization for pervasive multimedia," in *Proc. of the IEEE int. conf. on ubiquitous computing (UbiComp)*, Orange County, USA, pp. 422-440, 2006.
- [3] J. Hohn and F. Mattern, "Super-distributed RFID tag infrastructures," in *European symposium on ambient intelligence 2004*, Springer Berlin, pp. 1-12, 2004.
- [4] D. Hähnel, W. Burgard, D. Fox, K. Fishkin, and M. Philipose, "Mapping and localization with RFID technology," in *Proc. of the IEEE int. conf. on robotics and automation (ICRA)*, New Orleans, USA, pp. 1015-1020, 2004.
doi: [10.1109/ROBOT.2004.1307283](https://doi.org/10.1109/ROBOT.2004.1307283)
- [5] D. Joho, C. Plagemann, and W. Burgard, "Modeling RFID signal strength and tag detection for localization and mapping," in *Proc. of the IEEE int. conf. on robotics and automation (ICRA)*, Kobe, Japan, pp. 3160-3165, 2009.
doi: [10.1109/ROBOT.2009.5152372](https://doi.org/10.1109/ROBOT.2009.5152372)
- [6] T. Germa, F. Lerasle, N. Ouadah, V. Cadenat, and M. Devy, "Vision and RFID-based person tracking in crowds from a mobile robot," in *Proc. of the IEEE/RSJ int. conf. on intelligent robots and systems (IROS)*, St. Louis, USA, pp. 5591-5596, 2009.
doi: [10.1109/IROS.2009.5354475](https://doi.org/10.1109/IROS.2009.5354475)
- [7] A. Kleiner, J. Prediger, and B. Nebel, "RFID technology-based exploration and SLAM for search and rescue," in *Proc. of the IEEE/RSJ int. conf. on intelligent robots and systems (IROS)*, Beijing, China, pp. 4054-4059, 2006.
doi: [10.1109/IROS.2006.281867](https://doi.org/10.1109/IROS.2006.281867)
- [8] T. Raff and F. Allgöwer, "An EKF-based observer for nonlinear time-delay systems," in *Proc. of the 2006 american control conference*, Minneapolis, USA, pp. 3130-3133, 2006.
doi: [10.1109/ACC.2006.1657198](https://doi.org/10.1109/ACC.2006.1657198)
- [9] R. Johansson and A. Saffiotti, "Navigating by stigmergy: A realization on an RFID oor for minimalistic robots," in *Proc. of the IEEE int. conf. on robotics and automation (ICRA)*, Kobe, Japan, pp. 245-252, 2009.
- [10] P. Vorst and A. Zell, "Fully autonomous trajectory estimation with long-range passive RFID," in *Proc. of the IEEE int. conf. on robotics and automation (ICRA)*, Anchorage, USA, pp. 1867-1872, 2010.
doi: [10.1109/ROBOT.2010.5509810](https://doi.org/10.1109/ROBOT.2010.5509810)
- [11] J. F. Chen and C. C. Wang, "Simultaneous localization and mapping using a short-range passive RFID reader with sparse tags in large environments," in *Proc. of the IEEE workshop on advanced robotics and its social impacts (ARSO)*, Seoul, Korea, pp. 136-141, 2010.
doi: [10.1109/ARSO.2010.5680012](https://doi.org/10.1109/ARSO.2010.5680012)
- [12] P. Vorst, S. Schneegans, B. Yang, and A. Zell, "Self-localization with RFID snapshots in densely tagged environments," in *Proc. of the IEEE/RSJ int. conf. on intelligent robots and systems (IROS)*, Nice, France, pp. 1353-1358, 2008.
doi: [10.1109/IROS.2008.4650715](https://doi.org/10.1109/IROS.2008.4650715)
- [13] P. Vorst and A. Zell, "Particle filter-based trajectory estimation with passive UHF RFID fingerprints in unknown environments," in *Proc. of the IEEE/RSJ int. conf. on intelligent robots and systems (IROS)*, St. Louis, USA, pp. 395-401, 2009.
doi: [10.1109/IROS.2009.5354627](https://doi.org/10.1109/IROS.2009.5354627)
- [14] P. Vorst and A. Zell, "Semi-autonomous learning of an RFID sensor model for mobile robot self-localization," in *European symposium on ambient intelligence 2008*, Springer Berlin, pp. 273-282, 2008.
doi: [10.1007/978-3-540-78317-6_28](https://doi.org/10.1007/978-3-540-78317-6_28)
- [15] D. Sun, A. Kleiner, and T. Wendt, "Multi-robot range-only SLAM by active sensor nodes for urban search and rescue," in *Robocup 2008: Robot soccer world cup xii*, Springer Berlin, 2009, pp. 318-330.



- doi: [10.1007/978-3-642-02921-9_28](https://doi.org/10.1007/978-3-642-02921-9_28)
- [16] R. M. Eustice, H. Singh, and J. Leonard, "Exactly sparse delayed-state filters for view-based SLAM," *IEEE Transactions on Robotics*, vol. 22, no. 6, pp. 1100-1114, 2006.
doi: [10.1109/TRO.2006.886264](https://doi.org/10.1109/TRO.2006.886264)
- [17] S. J. Julier and J. K. Uhlmann, "A counter example to the theory of simultaneous localization and map building," in *Proc. of the IEEE int. conf. on robotics and automation (ICRA)*, Seoul, Korea, pp. 4238-4243, 2001.
doi: [10.1109/ROBOT.2001.933280](https://doi.org/10.1109/ROBOT.2001.933280)
- [18] J. Castellanos, J. Neira and J. Tardós, "Limits to the consistency of EKF-based SLAM," in *5th IFAC symp. on intelligent autonomous vehicles (IAV'04)*, Lisbon, Portugal, 2004.
- [19] J. Castellanos, R. Martinez-Cantin, J. Tardós, and J. Neira, "Robocentric map joining: Improving the consistency of EKF-SLAM," *Robotics and Autonomous Systems*, vol. 55, no. 1, pp. 21-29, 2007.
- [20] T. Bailey, J. Nieto, J. Guivant, M. Stevens, and E. Nebot, "Consistency of the ekf-slam algorithm," in *Proc. of the IEEE/RSJ int. conf. on intelligent robots and systems (IROS)*, Beijing, China, 2006, pp. 3562-3568.
doi: [10.1109/IROS.2006.281644](https://doi.org/10.1109/IROS.2006.281644)
- [21] S. Huang, G. Dissanayake, "Convergence and consistency analysis for extended kalman filter based SLAM," *IEEE Transactions on Robotics*, vol. 23, no. 5, pp. 1036-1049, 2007.
doi: [10.1109/TRO.2007.903811](https://doi.org/10.1109/TRO.2007.903811)
- [22] G. Agamennoni, J. Nieto, and E. Nebot, "An outlier-robust kalman filter," In *Proc. of the IEEE int. conf. on robotics and automation (ICRA)*, Shanghai, China pp. 1551-1558, 2011,.
- [23] W. S. Choi and S. Y. Oh, "Robust EKF-SLAM method against disturbance using the shifted mean based covariance inflation technique," In *Proc. of the IEEE int. conf. on robotics and automation (ICRA)*, Shanghai, China, pp. 4054-4059, 2011.
doi: [10.1109/ICRA.2011.5979735](https://doi.org/10.1109/ICRA.2011.5979735)
- [24] S. Thrun, W. Burgard, and D. Fox, "Probabilistic robotics," chap. 5, MIT Press, 2005.
- [25] F. Lu and E. Milios, "Robot pose estimation in unknown environments by matching 2d range scans," *Journal of Intelligent and Robotics Systems*, vol. 18, no. 3, pp. 249-275, 1997.
- [26] A. Koch and A. Zell, "Mapping of passive UHF RFID tags with a mobile robot using outlier detection and negative information," in *Proc. of the IEEE int. conf. on robotics and automation (ICRA)*, Hong Kong, China, pp.1619-1624, 2014.
doi: [10.1109/ICRA.2014.6907068](https://doi.org/10.1109/ICRA.2014.6907068)

